JOURNAL OF PHYSICAL ORGANIC CHEMISTRY
J. Phys. Org. Chem. **12**, 293–307 (1999)

Hydrogen bonding interactions between Starburst dendrimers and several molecules of biological interest

Marisa Santo and Marye Anne Fox*

Department of Chemistry, University of Texas at Austin, Austin, Texas 78712, USA

Received 19 December 1997; revised 18 March 1998; accepted 26 March 1998

ABSTRACT: ^{1}H NMR spectroscopy was used to analyze the interactions between poly(amidoamine) (PAMAM) Starburst dendrimers (SBDs) **1–4** and several biologically important guests (pyridine, quinoline, quinazoline, nicotine and trimethadione). Association constants obtained from changes in the chemical shifts of the amide protons in the host indicate two different interaction sites inside and on the periphery of the dendrimer. Binding at the inner site is inhibited in the ester-terminated dendrimers. Copyright © 1998 John Wiley & Sons, Ltd.

KEYWORDS: Starburst dendrimers; hydrogenbonding

INTRODUCTION

The poly(amidoamine) (PAMAM) Starburst dendrimers (SBDs) are of particular interest because their internal poly(amidoamine) structure may mimic the three-dimensional structure of biomacromolecules, such as proteins or enzymes.[1] In addition, such compounds also manifest high affinity toward external agents with complementary hydrogen bonding moieties, enabling them to function as effective molecular hosts.

Dendrimers possess three distinguishing architectural components:[2] (a) a unique core; (b) an interior consisting of repeat units of varying number, radially attached to the core; and (c) an exterior terminal functionality attached at the outermost position along the chain. The dendrimers studied here have an ethylenediamine (EDA) core to which four groups are attached. This structural feature determines the number of branches possible in the oligomeric intermediates. The interior layers here consist of repeat units formally derived from *N*-(2-aminoethyl) acrylamide (CH_2=CH(C=O)NH$CH_2CH_2NH_2$). The terminal group is either an *N*-(2-amino)acrylamide as in **1** and **2** or an acrylic ester as in **3** and **4** (Fig. 1).

Recently, photophysical probes have been used to characterize the interactions between guests included within a dendrimer and a reaction partner outside the complex. For example, electron-transfer quenching of photoexcited Ru(bypy)$_3^{2+}$ by methyl viologen has been used to investigate the structural differences between several different generations of Starburst dendrimers,[3,4] and a similar photophysical investigation of the interactions of an SBD with anionic and cationic surfactants has been carried out.[5] Pyrene has been used as a photoluminescence probe to explore the various hydrophobic sites in the microheterogeneous architecture in dendrimers analogous to **3** and **4**.[6] These studies implicate a change in morphology from an open, branched structure for short chains such **1–4** to a closed, increasingly compact surface for more extended chains. The low molecular weight dendrimers analogous to **1–4** appear to be hydrophilic, with large separations between the terminal groups. Such end-terminated dendrimers have been described as model anionic micelles.[3,6,7]

In addition, the structures of Cu(II) complexes formed with ester-terminated dendrimers in aqueous solution have been used to study host–guest interactions in the SBDs. For dendrimers of a length comparable to **1–4**, both the carboxylic groups at the dendrimer surface and the internal amido groups act as active complexation sites.[8] PAMAM-SBDs, when used as stationary phases in electrokinetic chromatography,[9] also showed skeleton selectivity and a clear preference for aromatic compounds, especially for rigid planar polynuclear aromatic hydrocarbons.

The SBDs **1–4** present two active sites for potential complexation with hydrogen bonding partners: the external surfaces of **1** and **2** are characterized by free amino groups, whereas dendrimers **1–4** all contain internal amido groups. In this study, we characterized the sites by ^{1}H NMR spectroscopy to analyze the interactions between each dendrimer and a complementary biologically active complexant, such as pyridine, quinoline, quinazoline, nicotine or trimethadione. Such studies can evaluate these dendrimers as hosts for biomacromolecular guests and can be used to predict their utility as carriers or stationary phases in chromatography.

**Correspondence to:* M. A. Fox, Department of Chemistry, University of Texas at Austin, Austin, Texas 78712, USA.
Contract/grant sponsor: Robert A. Welch Foundation.

 CCC 0894–3230/99/040293–15 $17.50

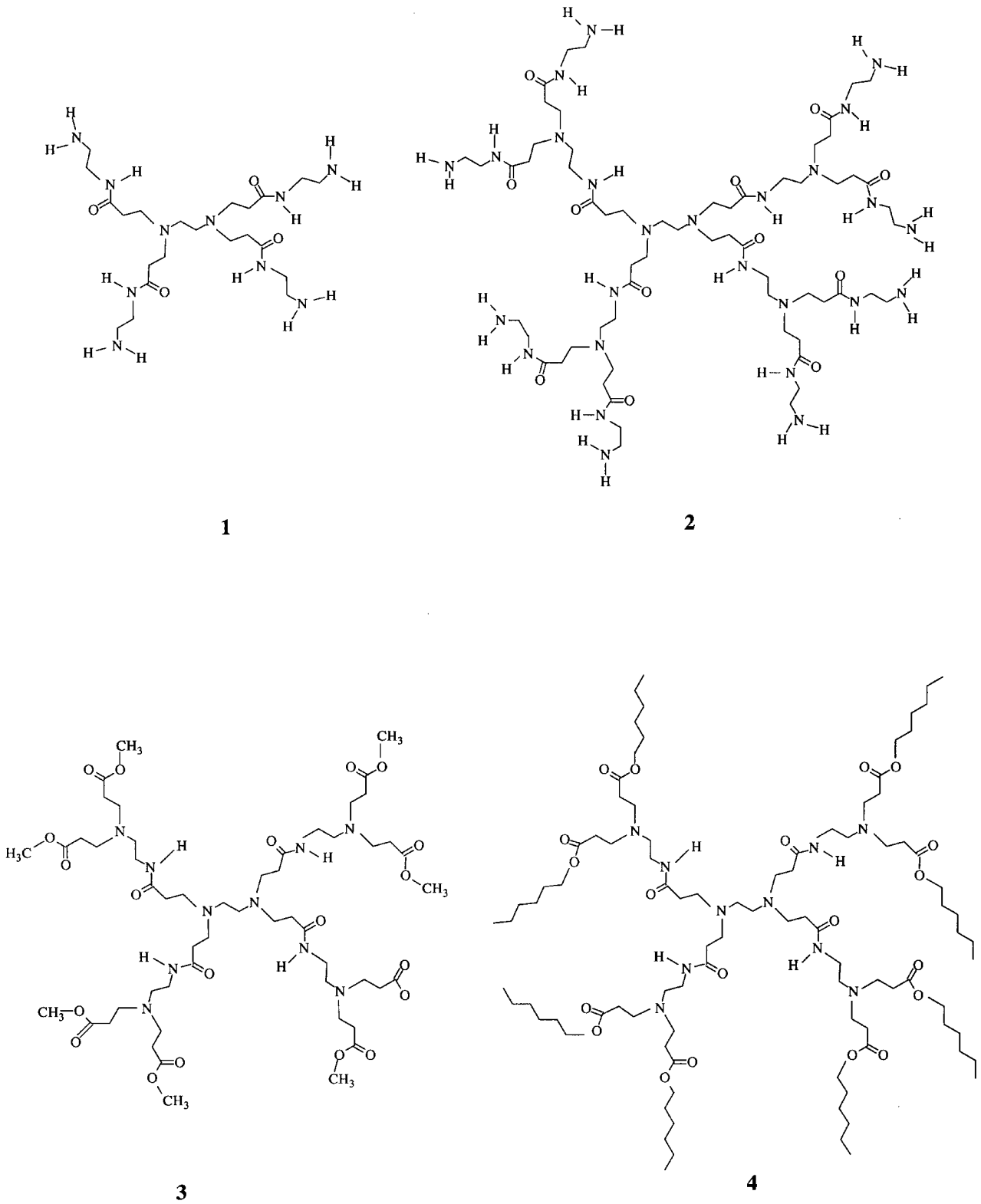

Figure 1. Poly(amidoamine) Starburst dendrimers employed as hosts

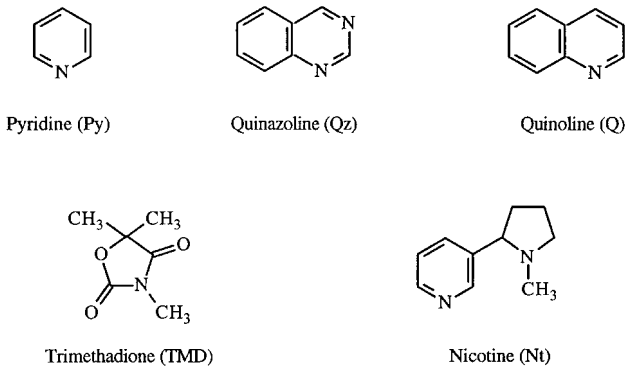

Figure 2. Guest probe molecules used in this study

The guest probes employed here (Fig. 2) were chosen because of their established reactivity as hydrogen bond acceptors.[10] The study of hydrogen bonding interactions between these pharmacological active compounds and biomacromolecules is important because they probe directly the non-covalent interactions that have been shown to be physiologically significant.

The present investigation focused on ^{1}H NMR shifts of the included molecules induced by dendrimers **1–4**. It addressed (1) the complexation of the SBDs with the probe molecule, and how solvent influences the strength of these interactions, (2) a quantitative determination of the energetic gain associated with hydrogen bonding between the SBD and the probe and (3) the effect of the chain length of the SBD on the character of the host–guest interactions.

EXPERIMENTAL

Materials. Dendrimers **1** and **2** were obtained from Aldrich as 20% methanol solutions. They were purified by evaporation of the solvent and by washing with acetone and diethyl ether. The product was stored in chloroform over type 4A molecular sieve beads of 8–12 mesh (EM Science) for 24 h. The chloroform was then removed by rotary evaporation between room temperature and 50 °C.

Quinazoline (Aldrich, 99%), nicotine (Aldrich, 99%), 3,5,5-trimethyloxalidine-2,4-dione (Sigma, 98%) and pyridine (Norell, 99.8%) were used as received. Quinoline (Kodak) was distilled under vacuum.

The deuterated solvents $CDCl_3$ (99.8 at% D) (Isotec), acetone (99.9 at% D) (Norell), methanol (99.8 at% D) (Sigma), water (99.8 at% D) (Norell), cyclohexene (99.5 at% D) (Sigma), toluene (99 at% D) (Sigma) and benzene (99.6 at% D) (Isotec) were used as received. Tetramethylsilane (99.9+% NMR grade, Aldrich) was used as an internal standard.

*Synthesis of dendrimer **3**.* To a 50 ml round-bottomed flask was added 5.0 g of a solution of **1** (20% in MeOH). The methanol was evaporated at room temperature and methyl acrylate (1.7 g, 19 mmol) was added along with 2.7 g MeOH (50% solution by weight). This solution was stirred for 48 h at room temperature. MeOH and excess methyl acrylate were removed by rotary evaporation between room temperature and 40 °C, yielding 0.65 mmol (33%) of a colorless oil. ^{1}H NMR data are listed in Table 1.

Table 1. Proton chemical shift assignments for ester-terminated Starburst dendrimers **3** and **4** in $CDCl_3$

Dendrimer	Structure	Assignments (δ, ppm)[a]
3	(**a**) (**b**) (**c**) (**d**) (**e**) (**f**) (**h**) (**i**) (**j**) $-[CH_2-N(CH_2CH_2CONH-CH_2CH_2-N(CH_2CH_2CO_2CH_3)_2]_2$	(**a**), (**f**) 2.55 (m) (**b**), (**h**) 2.77 (m) (**c**) 2.36 (5) (d) 7.21 (bt) (**e**) 3.28 (m) (**i**) 2.44 (t) (**j**) 3.67 (s)
4	(**a**) (**b**) (**c**) (**d**) (**e**) (**f**) (**h**) (**i**) $-[CH_2-N(CH_2CH_2CONH-CH_2CH_2-N(CH_2CH_2CO_2R_2)_2]_2$ (**k**) (**l**) (**m**) (**n**) $R=-CH_2-CH_2-(CH_2)_3-CH_3$	(**a**), (**f**) 2.55–2.50 (m) (**b**), (**h**) 2.78 (m) (**c**) 2.35 (t) (**d**) 7.21 (bt) (**e**) 3.28 (m) (**i**) 2.43 (t) (**k**) 4.05 (t) (**l**) 1.31 (m) (**m**) 1.62 (m) (**n**) 0.89 (t)

[a] (m) = multiplet, (bt) = broad triple, (bs) = broad singlet.

Table 2. Proton chemical shift assignments for amino-terminated Starburst dendrimers **1** and **2** in $CDCl_3$

Dendrimer	Structure	Assignments (δ, ppm)[a]
1	(**a**) (**b**) (**c**) (**d**) (**e**) (**f**) (**g**) $-[CH_2-N(CH_2CH_2CONH-CH_2CH_2-NH_2)_2]_2$	(**a**) 2.40 (m) (**b**) 2.66 (m) (**c**) 2.34 (m) (**d**) 7.54 (bt) (**e**) 3.26 (m) (**f**) 2.81 (m) (**g**) 1.40 (bs)
2	(**a**) (**b**) (**c**) (**d**) (**e**) (**f**) (**h**) (**i**) (**o**) (**p**) (**q**) (**r**) $-[CH_2-N(CH_2CH_2CONH-CH_2CH_2-N(CH_2CH_2CONH-CH_2-CH_2-NH_2)_2]_2$	(**a**), (**f**) 2.51 (m) (**b**), (**h**) 2.73 (m) (**c**), (**i**) 2.36 (m) (**d**) 8.05 (bt) (**e**) 3.23 (m) (**o**) 7.73 (bt) (**p**) 3.29 (m) (**q**) 2.82 (m) (**r**) 1.74 (s)

[a] (m) = multiplet, (bt) = broad triple, (bs) = broad singlet.

*Synthesis of dendrimer **4**.* To a 50 ml round-bottomed flask was added 5.0 g of a solution of **1** (20% in MeOH). The methanol was evaporated room temperature and hexyl acrylate (3.8 g, 24 mmol) was added along with 5.1 g of hexan-1-ol (50% solution by weight). This solution was stirred for 48 h at 50 °C under argon. Hexanol and excess hexyl acrylate were removed by rotary evaporation between room temperature and 80 °C.

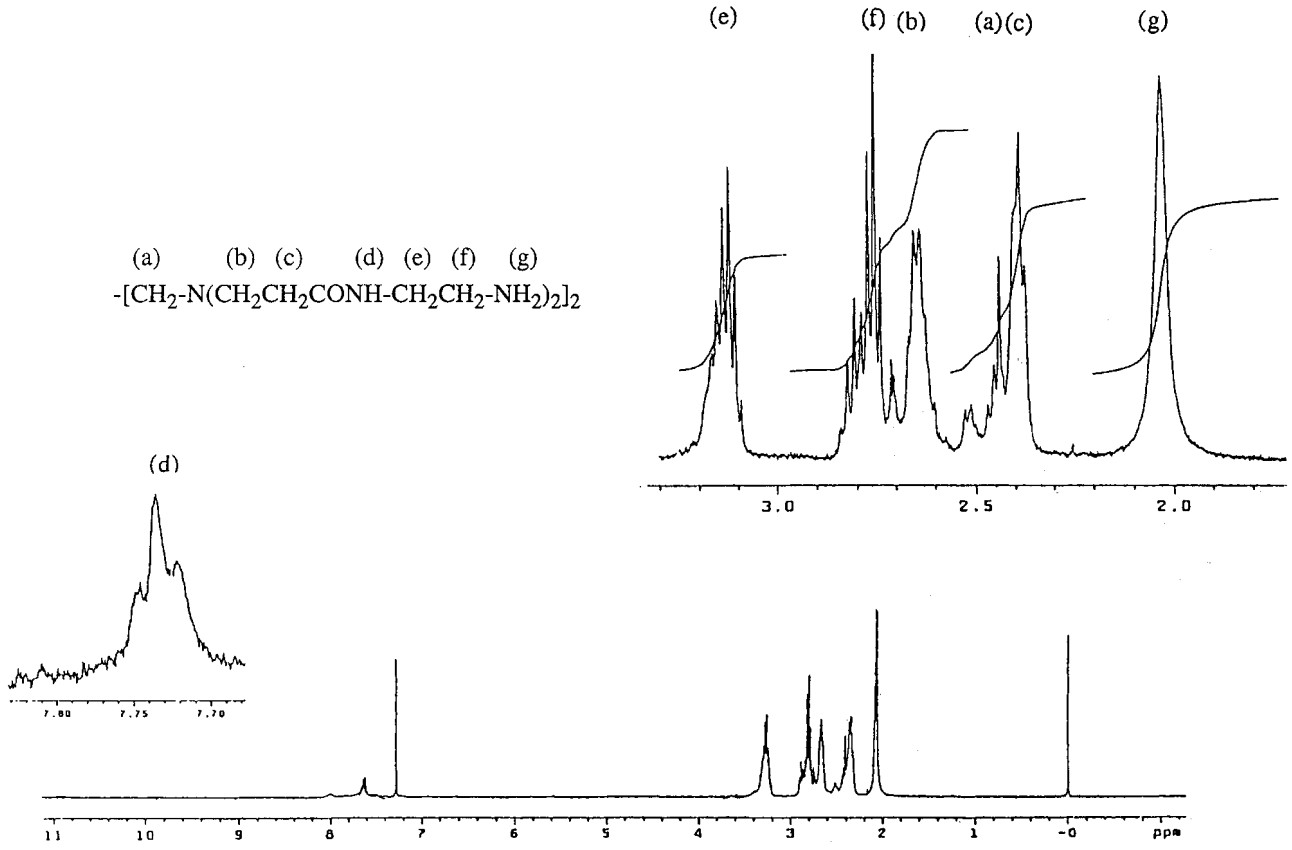

Figure 3. ^1H NMR spectra at 293 K of **1** in $CDCl_3$ (10^{-2} M)

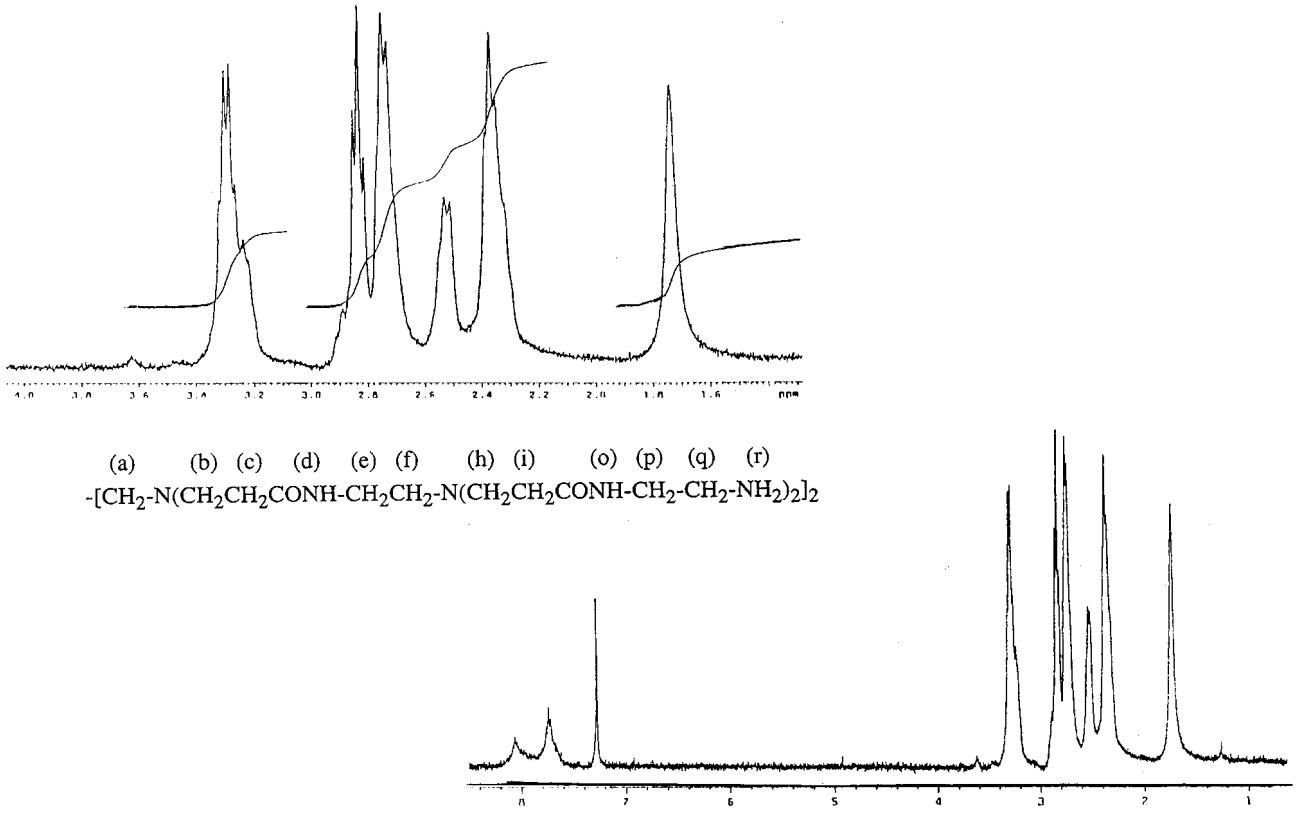

Figure 4. ^{1}H NMR spectra at 293 K of **2** in $CDCl_3$ (10^{-2} M)

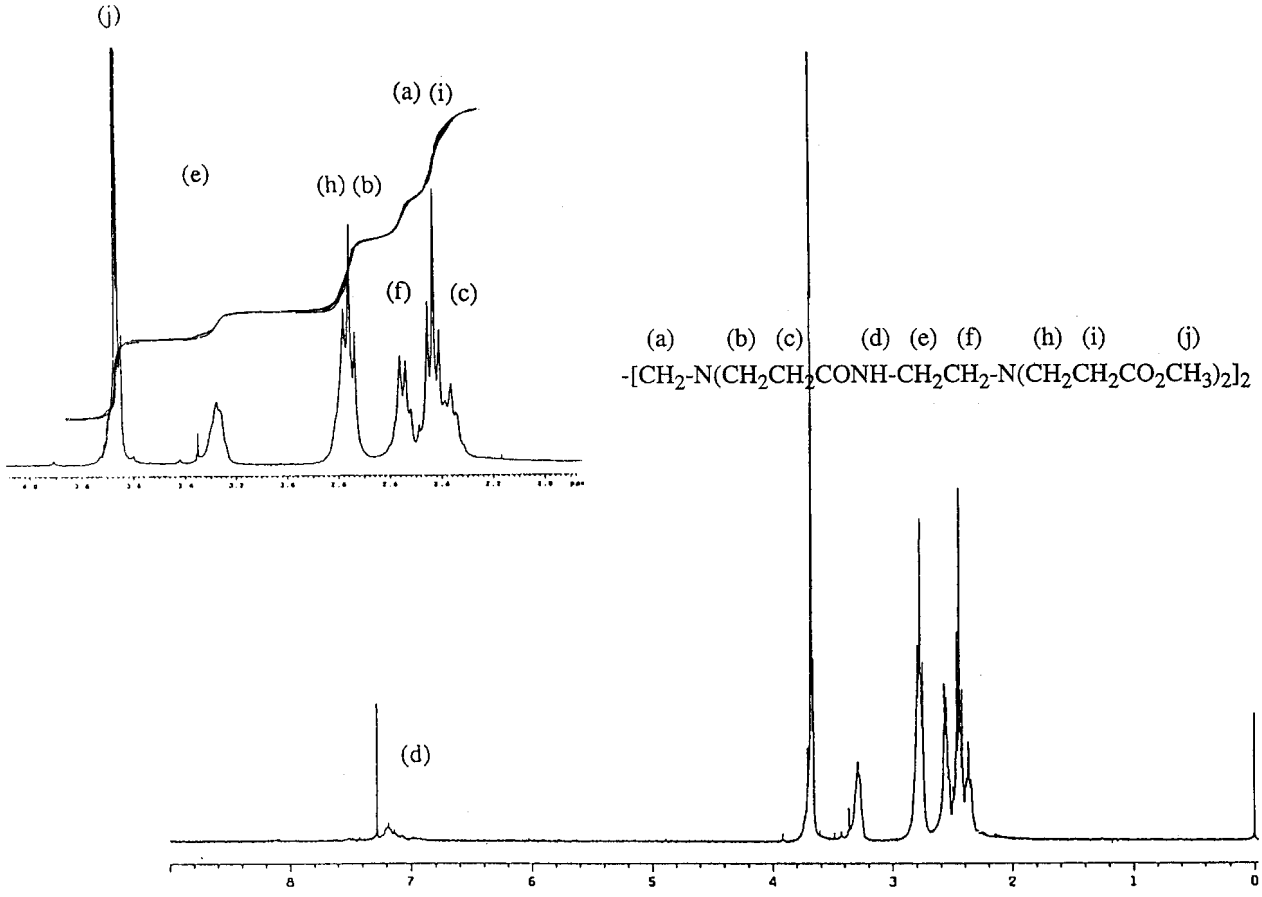

Figure 5. ^{1}H NMR spectra at 293 K of **3** in $CDCl_3$ (10^{-2} M)

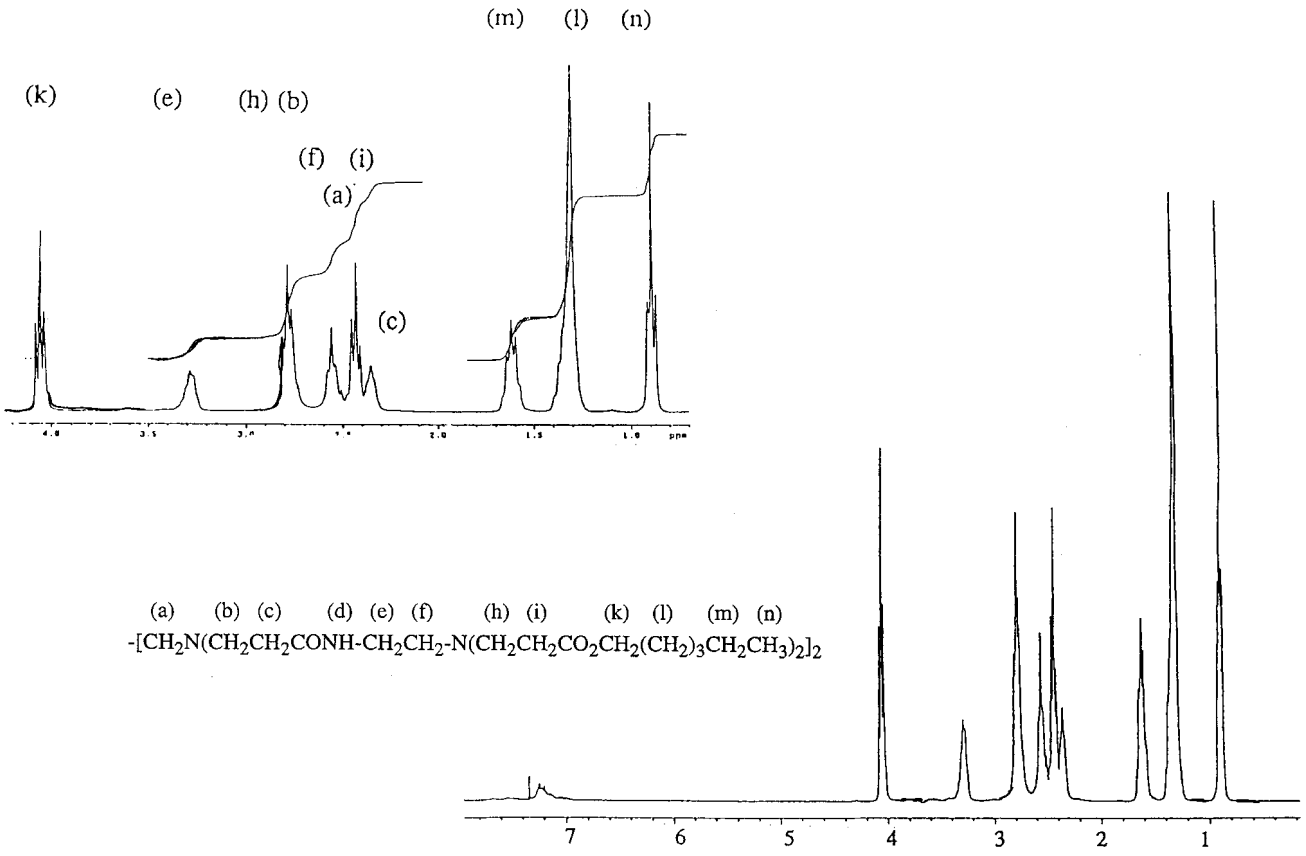

Figure 6. ^{1}H NMR spectra at 293 K of **4** in $CDCl_3$ (10^{-2} M)

A colorless oil, 0.42 mmol (21%), was obtained. ^{1}H NMR data are listed in Table 2.

Methods. ^{1}H NMR spectra were obtained on a Varian 300 Hz spectrometer with tetramethylsilane as internal standard at 293 K in chloroform. Probe concentrations were varied in the concentration range 10^{-2}–1 M at a constant concentration of the SBD ($<10^{-2}$ M). NMR spectra were recorded 1–2 h after preparation of the samples and all the solutions were refrigerated immediately after preparation.

RESULTS AND DISCUSSION

Assignment of chemical shifts in dendrimer complexes

Assigning each proton of dendrimers **1–4** is critical because the shift of each signal must be used to define the zone of interaction. The assignments were based on ^{1}H and ^{13}C one-dimensional NMR spectra and COSY 1H/^{1}H, HMQC ^{13}C/^{1}H NMR spectra. One-dimensional 1H NMR spectra for **1–4** (Figs 3–6) show three kinds of protons: the amide protons at low field (triplet, δ = 7.54 ppm), amine protons at high field (singlet, δ = 1.39 ppm) and the methylene protons adjacent to the amide group at a much lower field than the others methylenes (multiplet, δ = 3.26 ppm). Between δ 3.0 and 2.3 ppm are found the signals of the others methylenes, which were assigned by analysis of the corresponding two-dimensional NMR spectra (Figs 7–10).

In the homonuclear correlation spectroscopy (COSY) spectrum of **1** (Fig. 7), interaction between the different protons in the molecule permitted assignment of methylenes **f**, which show interaction with the methylene **d** protons. In contrast, methylenes **a** show no interaction with other protons in the molecule. Heteronuclear multiple-quantum coherence (HMQC) spectra reveal all the expected cross peaks from the secondary and tertiary carbons,[11] making it possible to assign the **b** and **c** methylene protons. The ^{13}C signal of the **c** methylene, next to an amide group, is at lower frequency than the ^{13}C signal of the **b** methylene adjacent to an amino group. Following the connectivities [broken lines in Fig. 7(B)], a full assignment can be made.

Two types of amide proton signals were found in **2:** an internal amide at δ 8.06 ppm and an external amide at δ 7.50 ppm. This assignment was confirmed by HQMC, 13C/^{1}H and ^{15}N/^{1}H two-dimensional NMR spectroscopy [Fig. 10(b) and (c)].

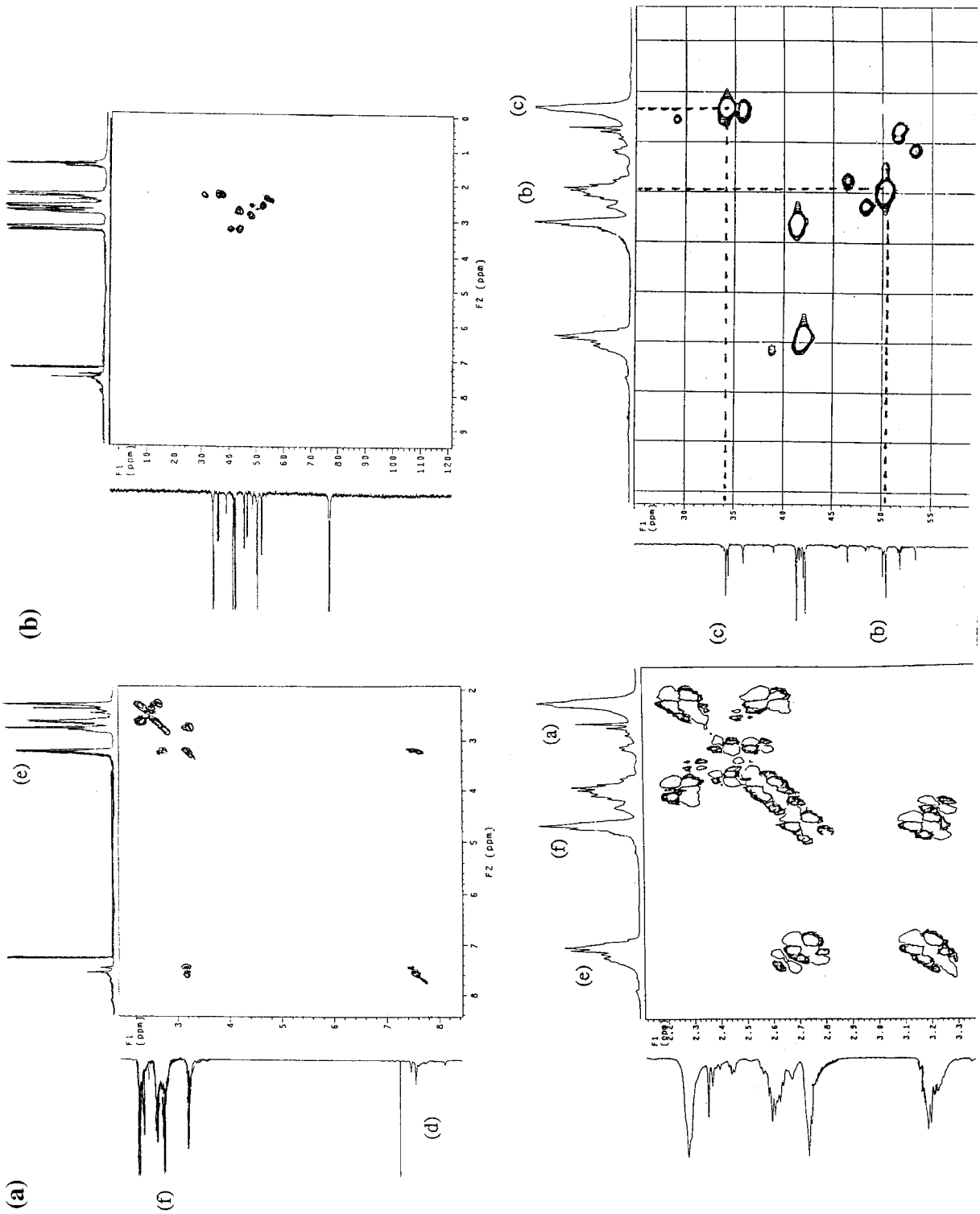

Figure 7. (A) Two-dimensional (H,H COSY) NMR spectra of **1** in $CDCl_3$ (10^{-2} M) at 300 K; (B) two-dimensional (HMQC $^{13}C/^{1}H$) NMR spectra of **1** in $CDCl_3$ (10^{-2} M) at 300 K. Peak assignments as shown in Fig. 3

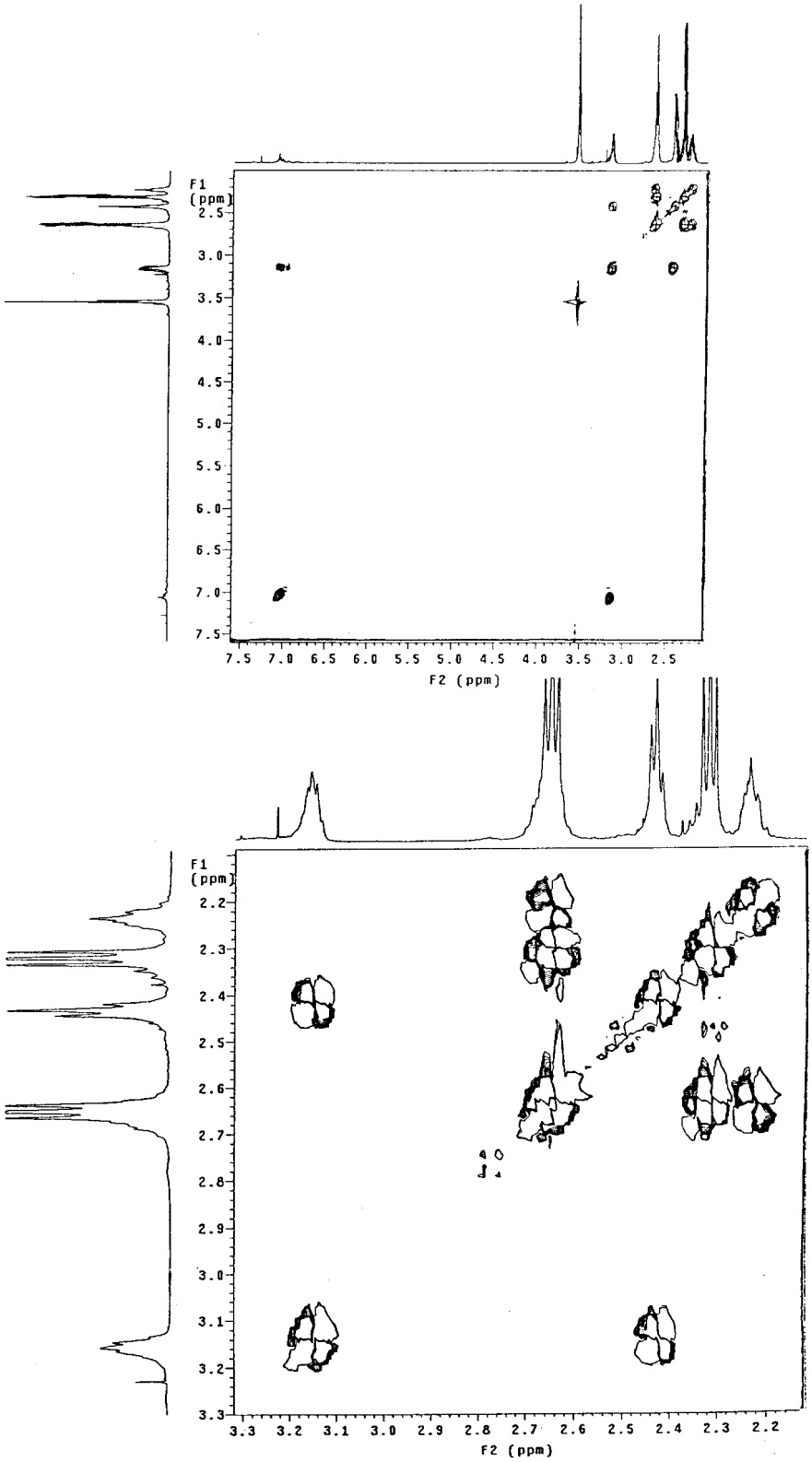

Figure 8. Two-dimensional (H,H COSY) NMR spectra of **3** in $CDCl_3$ (10^{-2} M) at 300 K. Peak assignments as in Fig. 5

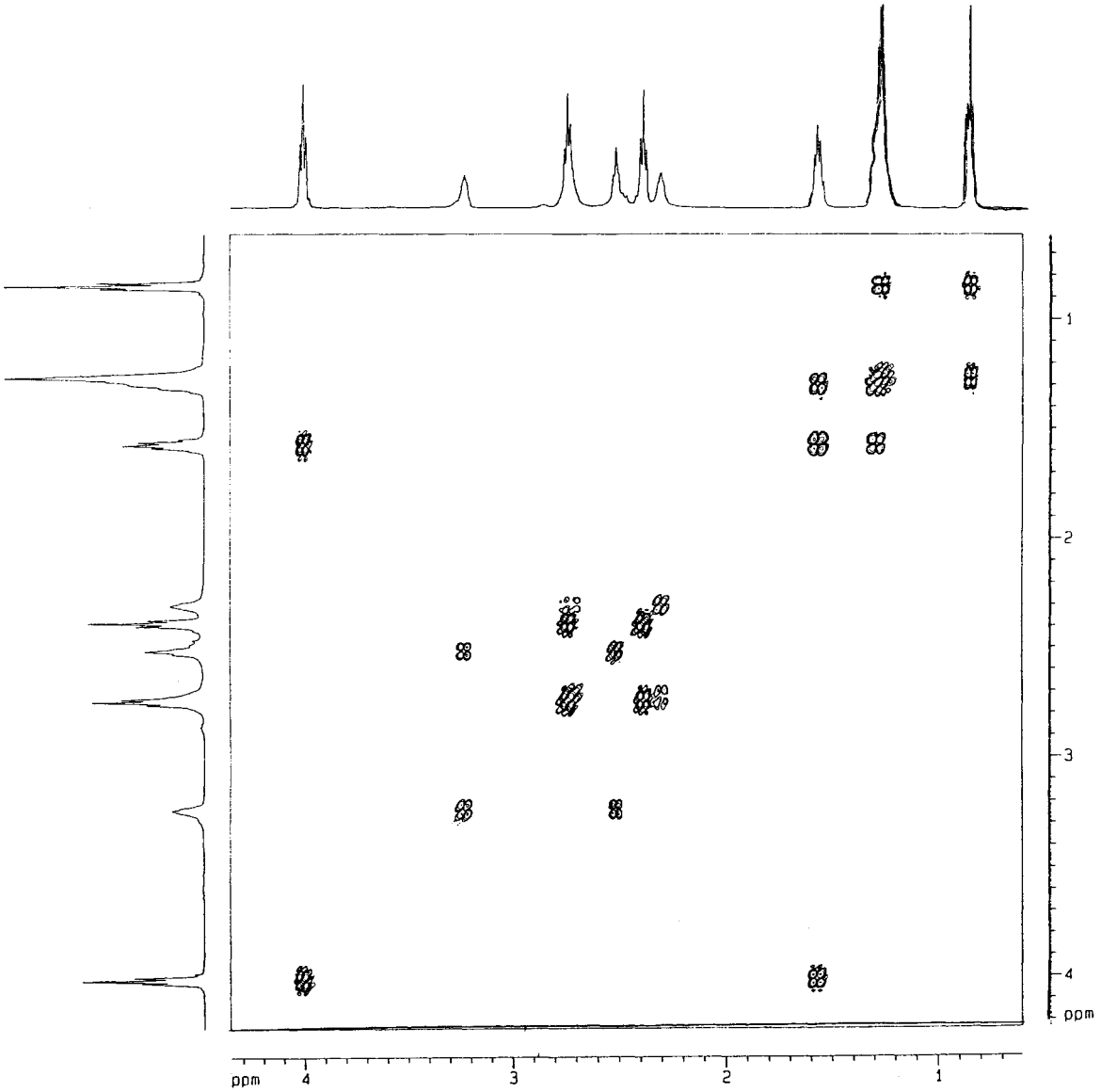

Figure 9. Two-dimensional (H,H COSY) NMR spectra of **4** in $CDCl_3$ (10^{-2} M) at 300 K. Peak assignments as in Fig. 6

Table 3. Chemical shifts of the protons of **1** induced by different solvents

	Characteristic[a]			^{1}H chemical shift (δ, ppm)[b,c]		
Solvent	π	β	α	Amide H (**d**)	CH_2 (**e**)	Amino H (**g**)
Chloroform	0.58	0	0.44	7.54	3.26	1.40
Acetone[c]	0.71	0.48	0.08	7.94	3.36	1.97
Methanol	0.60	0.62	0.93	—[d]	3.30	—[d]
Water	1.09	0.18	1.17	—[d]	3.30	—[d]
Pyridine	0.87	0.64	0	8.63	3.52	3.01

[a] π = Polarity, β = basicity, α = acidity.
[b] From tetramethylsilane as internal standard; assignments as in Table 2.
[c] Small contributions from imine formation with solvent were also observed, but are omitted for clarity.
[d] Vanished upon equilibration.

Table 4. ^{1}H chemical shifts of **3** induced by different solvents

	Characteristic[a]			Chemical shift (δ, ppm)[b]			
Solvent	π	β	α	Amide H (**d**)	CH_2 (**j**)	CH_2 (**e**)	CH_2 (**i**)
Chloroform	0.58	0	0.44	7.21	3.67	3.27	2.44
Acetone[c]	0.71	0.48	0.08	7.33	3.64	3.25	2.44
Methanol	0.60	0.62	0.93	—[d]	3.30	3.25	2.46
Water	1.09	0.18	1.17	—[d]	3.56	3.15	2.41
Pyridine	0.87	0.64	0	8.19	3.67	3.56	2.65
Benozene	0.59	0.10	0	7.48	3.51	3.43	2.65

[a] π = Polarity, β = basicity, α = acidity.
[b] From tetramethylsilane as internal standard; assignments as in Table 1.
[c] Small contributions from imine formation with solvent were also observed, but the peak positions are omitted for clarity.
[d] Vanished upon equilibration.

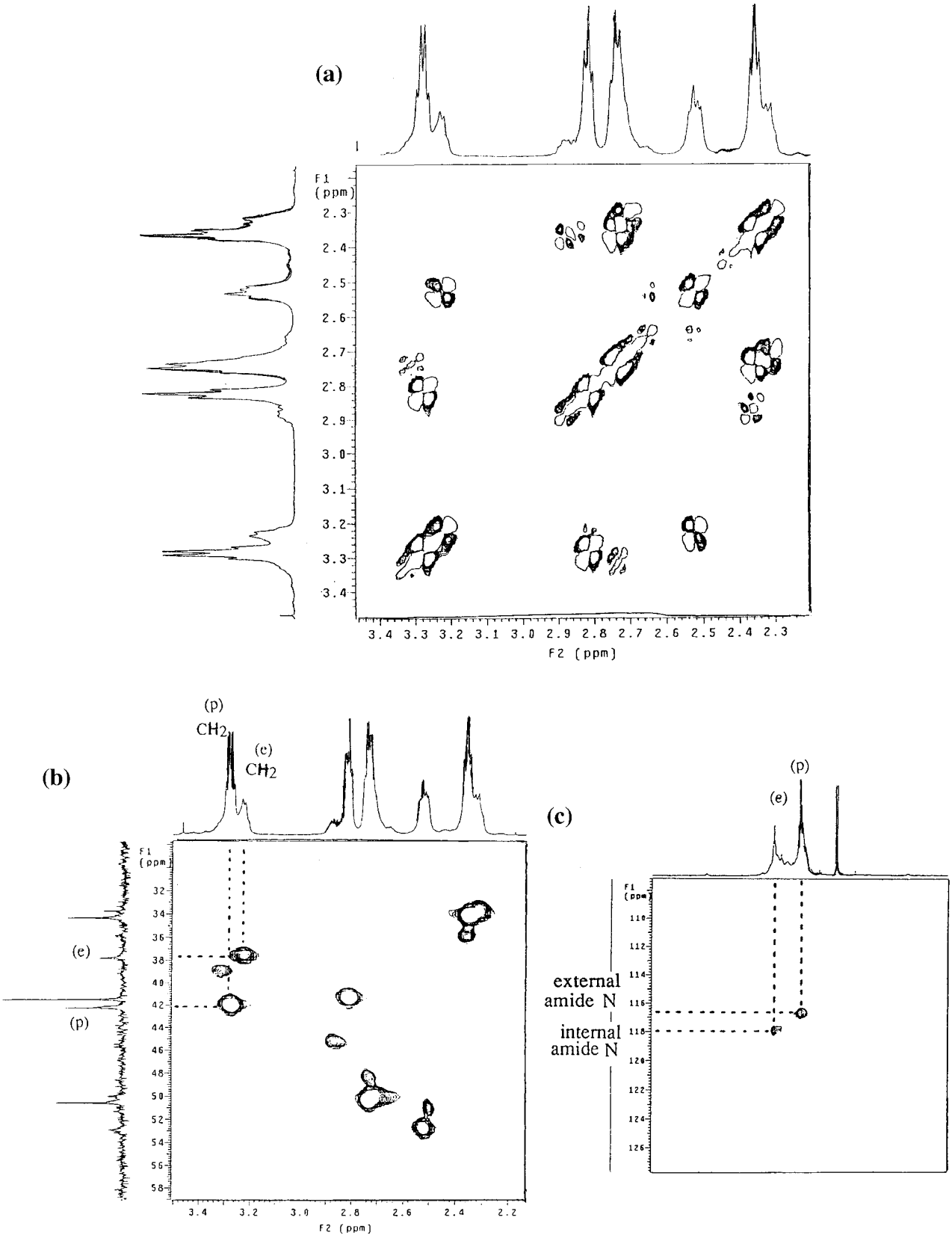

Figure 10. (a) Two-dimensional (H,H COSY) NMR spectra of **2** in $CDCl_3$ (10^{-2} M) at 300 K; (b) two-dimensional (HMQC $^{13}C/^{1}H$) NMR spectra and (c) (HMQC $^{15}N/^{1}H$) NMR spectra of **2** in $CDCl_3$ (10^{-2} M) at 300 K. Peak assignments as in Fig. 4

Table 5. ^{1}H chemical shifts of **4** induced by different solvents

Solvent	Characteristic[a]			Chemical shift (δ, ppm)[b]			
	π	β	α	Amide H	CH_2 (**k**)	CH_2 (**e**)	CH_2 (**i**)
Cyclohexane	−0.08	0	0	7.51	4.03	3.25	2.39
Chloroform	0.58	0	0.44	7.21	4.05	3.28	2.43
Acetone[c]	0.71	0.48	0.08	7.38	4.07	3.27	2.47
Methanol	0.60	0.62	0.93	—[d]	4.06	3.31	2.46
Water	1.09	0.18	1.17	—[d]	3.90	3.15	2.29
Pyridine	0.87	0.64	0	7.64	4.06	3.30	2.44
Benzene	0.59	0.10	0	7.50	4.06	3.44	

[a] π = Polarity, β = basicity, α = acidity.
[b] Against tetramethysilane as internal standard; assignments as in Table 1.
[c] Small contributions from imine formation with solvent were also observed, but are omitted for clarity.
[d] Vanished upon equilibration.

Solvent effects on the ^{1}H NMR spectra of 1–4

Solvents of different polarity, acidity and basicity (cyclohexane, benzene, toluene, chloroform, acetone, methanol, water and pyridine) induce different chemical shifts in **1–4**. The largest shifts were observed in the terminal amino group of **1**. The amine and the methylenic protons adjacent to the amide in the internal structure of **1** also shift with solvent (Table 3).

The amide protons in **1–4** vanish in water and methanol by exchange, but show large downfield shifts in hydrogen bond acceptor solvents, such as acetone or pyridine. Such shifts are normally associated with changes in the electronic density in the neighboring proton. The amino resonances also vanish in water and methanol, because of exchange, but a downfield shift is

Table 6. Association constants between pyridine and dendrimers **1–4**

Dendrimer	K_a (l mol^{-1}) amide H (**d**)	R[a]	K_a (l mol^{-1}) amine H (**g**)	R[a]
1	1.31	0.9968	0.36	0.9837
2	0.82	0.9598	0.16	0.9766
3	1.11	0.9617	—	
4	1.06	0.9466	—	

[a] Correlation coefficient.

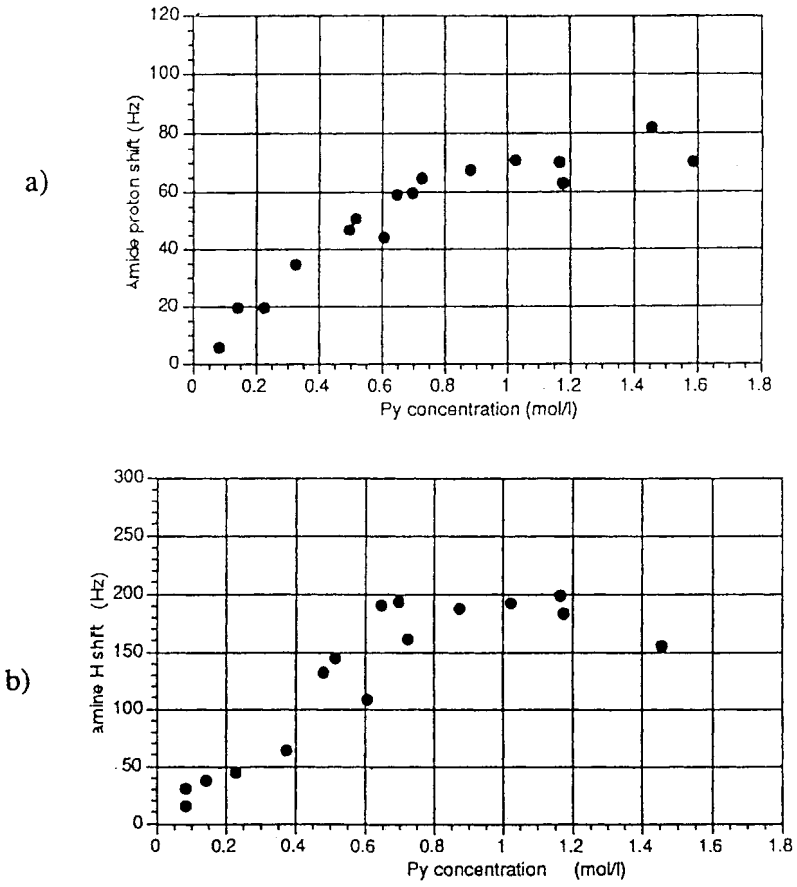

Figure 11. Changes in the ^{1}H NMR chemical shifts of **1** induced by increases in concentration of pyridine in $CDCl_3$: (a) amido group; (b) amino group

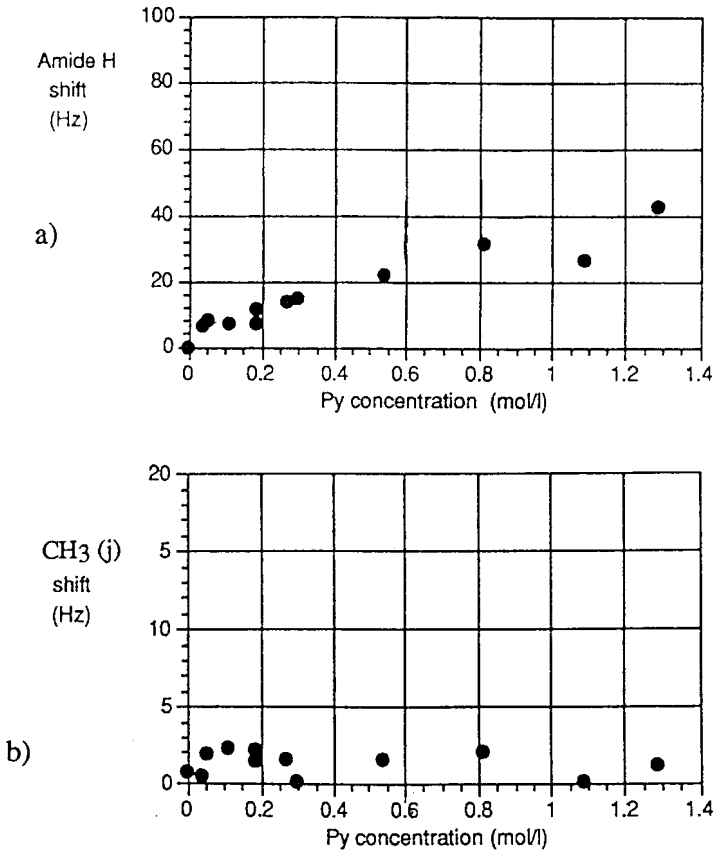

Figure 12. Changes in the ^{1}H NMR chemical shifts of **3** induced by increases in concentration of pyridine in $CDCl_3$: (a) amido group; (b) CH_3 (**j**) group

observed in solvents where the hydrogen bonding is present, such as pyridine and acetone (Table 3). The methylenic protons show only a small downfield shift, except in pyridine, where larger shifts have been attributed to aromatic solvent, i.e. the so-called aromatic solvent-induced shift effect.[12]

A similar study of solvent effects in **3** and **4** gave analogous results. The amide protons shift in the same

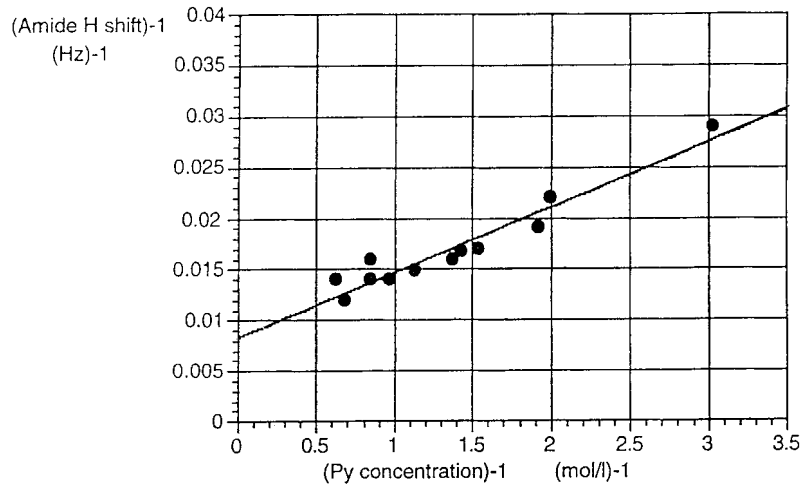

Figure 13. Interaction between the amide groups in dendrimer **1** and pyridine at 293 K in $CDCl_3$. [**1**] = 0.016 M; [pyridine] = 0.52–1.5 M. Association constant $K = 1.31$ l mol^{-1}

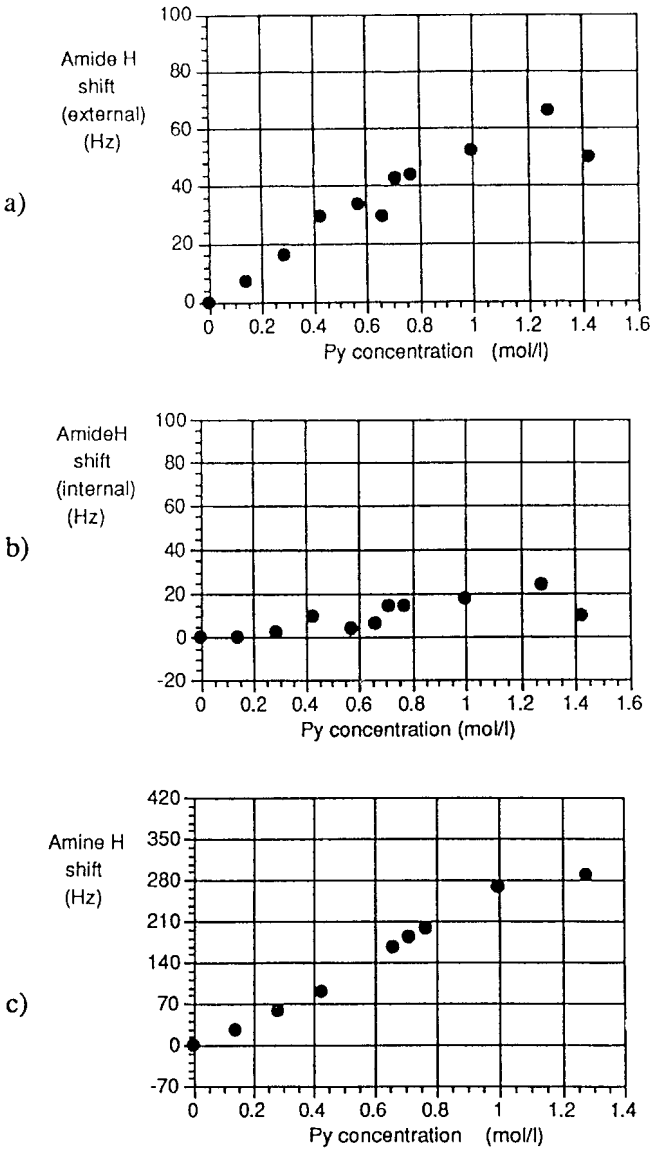

Figure 14. Changes in the ^{1}H NMR chemical shifts of **2** induced by increases in concentration of pyridine in $CDCl_3$: (a) external amido group; (b) internal amido group; (c) amino group

direction, and the shifts in the methylenic groups adjacent to the amino groups are much larger than those observed for the other methylenic protons (Tables 4 and 5).

Hydrogen bonding interactions

Assessment of equilibrium binding. The most significant ^{1}H chemical shift in an included guest is caused by strong hydrogen bonding interactions between a dendrimer amide proton and pyridine.

Consider the following equilibrium:

$$A - H + B \rightleftharpoons A - HB \quad (1)$$

where A—H is the amide proton and B is the pyridine nitrogen. If the formation of the hydrogen-bonded complex is fast, the observed chemical shift of the hydrogen bonding proton δ_{obs} will be a time-weighted average of the chemical shift of the protons in the complex $\delta_{(AH \cdots B)}$, and the chemical shift of the free molecule A—H, δ_f:[13]

$$\delta_{obs} = \frac{[AH]_0 - [AH \cdots B]}{[AH]_0}\delta_f + \frac{[AH \cdots B]}{[AH]_0}\delta_{AH \cdots B} \quad (2)$$

where $[AH]_0$ is the initial concentration of hydrogen bonding donor and $[AH \cdots B]$ is the complex concentration.

Rearranging Eqn 2 gives

$$[AH \cdots B] = \frac{\delta_{obs} - \delta_f}{\delta_{[AH \cdots B]} - \delta_f}[AH]_0 \quad (3)$$

By inserting these values, one obtains the following equilibrium expression:

$$K[AH]_0[B]_0 - K[AH \cdots B]\{[AH]_0 + [B]_0 - [AH \cdots B]\} = [AH \cdots B] \quad (4)$$

where K is the equilibrium constant and $[B]_0$ is the initial concentration of hydrogen bonding acceptor.

Combining Eqns 3 and 4 gives

$$\frac{[B]_0}{\Delta_{obs}} = \frac{1}{\Delta_{[AH \cdots B]}}\{[AH]_0 + [B]_0 - [AH \cdots B]\} + \frac{1}{K_{ass}\Delta_{[AH \cdots B]}} \quad (5)$$

where $\Delta_{obs} = \delta_{obs} - \delta_f$ and $\Delta[AH \cdots B] = \delta_c - \delta_f$. Equation 5 contains two unknowns, $[AH \cdots B]$ and δ_c, which can be calculated by an iterative procedure.[14] A plot of $[B]_0/\delta_{obs}$ versus $[A—H]_0 + [B]_0$ gives a line with a slope of $1/\Delta[AH \cdots B]$. This is then substituted into Eqn 3 to obtain an approximate value of $[AH \cdots B]$, which is then used in Eqn 5 to calculate an improved value of the slope. The procedure is repeated until two successive cycles yield identical values for the slope. The final value of the equilibrium constant is calculated from the limiting slope and intercept values. The value of δ_c is also obtained from the final slope.

If $[A—H]_0 <<< [B]_0$, Eqn 5 reduces to

$$\frac{1}{\Delta_{obs}} = \frac{1}{\Delta_{[AH \cdots B]}} + \frac{1}{K\Delta_{[AH \cdots B]}[B]_0} \quad (6)$$

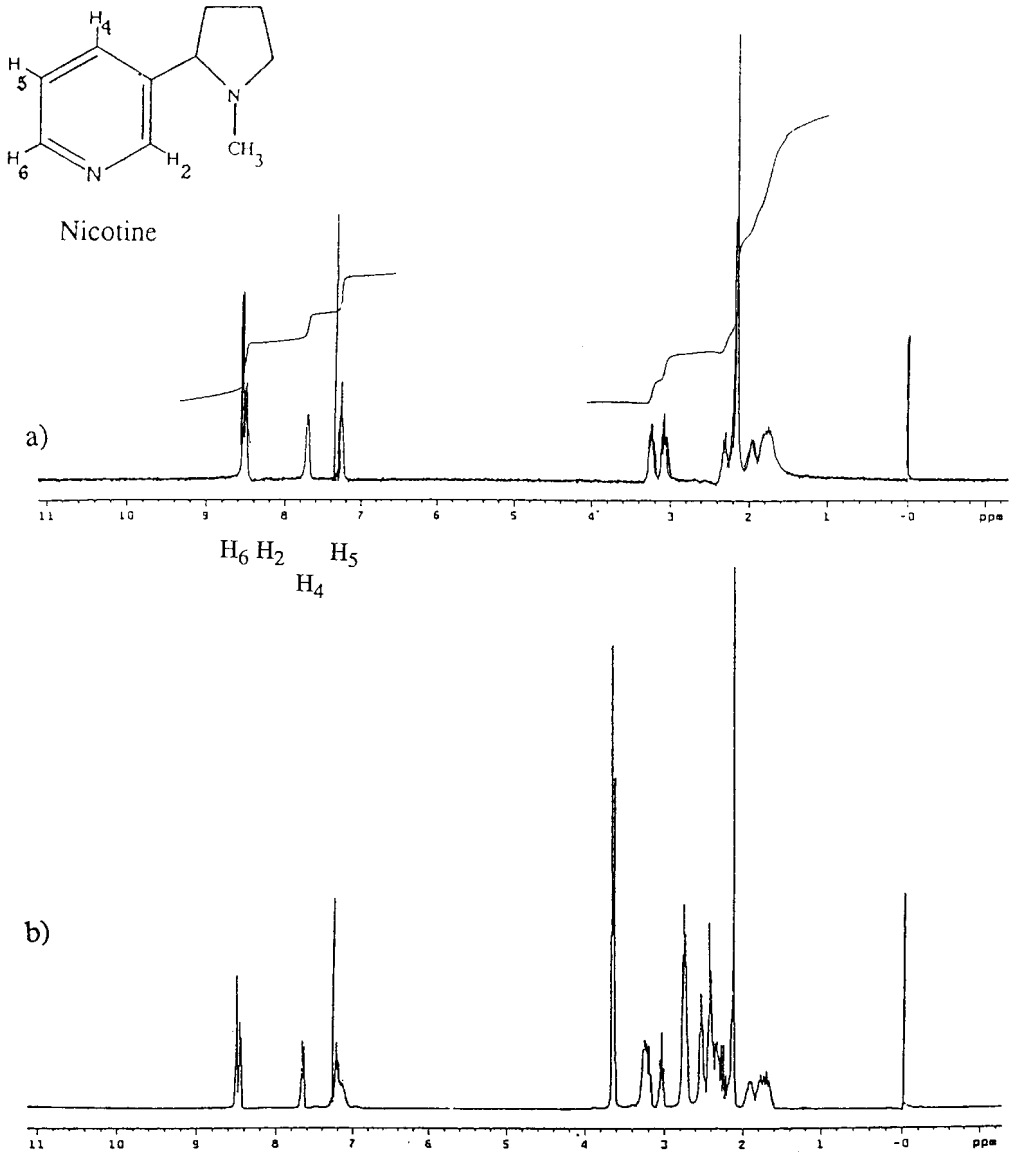

Figure 15. (a) ^{1}H NMR spectrum of nicotine; (b) ^{1}H NMR spectrum of nicotine with **3** in $CDCl_3$ at 293 K

Interaction of dendrimers 1, 2, 3, and 4 with pyridine. Changes in the ^{1}H NMR chemical shifts of **1**–**4** were induced by increasing the pyridine concentration. Dendrimer **1** shows two active regions the internal amido group and the external amino group (Fig. 11). Dendrimer **3** shows a strong interaction with pyridine only through the amide proton (Fig. 12).

Equation 6 was used to calculate the association constant between SBDs and pyridine in chloroform. This same equation can be used in systems with more than one hydrogen bonding donor site, but only if the concentration of the donor site is smaller than that of the acceptor i.e. if $\Sigma[A—H]_i <<< [B]_0$.[15]

Figure 13 illustrates a plot of Eqn 6 for **1**, providing the association constants K_a between **1** and pyridine (Table 6). The associations constants for **1** are larger than those for **3** or **4** because the length of the chain in these dendrimers makes difficult the migration of pyridine to the internal amide group where further association could take place.

Dendrimer **2** shows a primary interaction with pyridine along the external surface. Both the amine and amide groups show changes in proton shifts, but no interaction is found with the internal amide group proton (d) in Fig. 14. It is likely that in **2** the migration of pyridine to the inner groups of the dendrimer is more difficult (Table 6).

Interaction between SBDs and quinazoline and quinoline. The complexation of quinazoline and quinoline was attempted with those dendrimers which have

only one type of interactive amido proton (i.e. **3** and **4**). Equation 5 was then used to calculate the relevant association constant.

The interaction between **3** and these polycyclic acceptors give $K_a = 0.83$ l mol^{-1} and $K_a = 0.69$ l mol^{-1} with quinoline and quinazoline, respectively, in the same order as expected from the basicities of these acceptors.[16] In **4**, no interaction with quinazoline or quinoline is detectable, and no significant changes in ^{1}H chemical shifts are observed upon increasing the concentration of the acceptor. Presumably, the local tighter packing in dendrimer **4** is responsible for this difference, as percolation of these large heterocycles becomes more difficult.

Hydrogen bonding between 1–4 and trimethadione and nicotine. No significant interactions are observed between trimethadione and any of the dendrimers studied. The changes in the dendrimers' proton chemical shifts are consistently within experimental error.

In nicotine, the chemical shifts of the aromatic protons (H-4 and H-5) overlap with those of the amide protons in **1–4** (Fig. 15). This overlap makes it difficult to follow the amine proton shift of the dendritic molecule. Although H-6 in nicotine can be observed, no shift is observed when the concentration of nicotine is fixed and the concentration of dendrimer is increased or decreased. Thus, interactions between the SBD and the nicotine ring nitrogen are negligible, but binding at the other amino nitrogen is not unambiguously excluded. Changes in the chemical shift of the *N*-methyl protons of nicotine are observed, but they overlap with the aliphatic protons of the dendrimers, making quantitative study difficult.

CONCLUSIONS

Complexation with pyridine involves both the external and the internal sites only in those dendrimers terminated with amino groups. No proton shifts could be observed in the ester-terminated dendrimers **3** and **4**, indicating that pyridine did not complex with the external carboxylic ester.

Basic guests tend to bind with the amido group in the internal groups present in short dendritic branches. When long ester chains are present, hydrogen bonding between the internal amido group becomes difficult, and association constants become correspondingly small.

Acknowledgements

This work was supported by the Robert A. Welch Foundation. We thank Nick Crano for assistance with the synthesis of **3** and **4**. M.S. thanks the Universidad Nacional de Rio Cuarto for fellowship support that made possible her visit to Austin, where these measurements were made.

REFERENCES

1. M. F. Ottaviani, E. Cossu, N. Turro and D. A. Tomalia, *J. Am. Chem. Soc.* **117**, 4387 (1995).
2. D. A. Tomalia, H. Baker, J. Dewald, M. Hall, G. Kallos, S. Martin, J. Roeck, J. Ryder and P. Smith, *Polym. J.* **17**, 117 (1985).
3. K. Gopidas, A. Leheny, G. Caminati, N. Turro and D. Tomalia, *J. Am. Chem. Soc.* **113**, 7335 (1991).
4. M. C. Moreno-Bondi, G. Orellana, N. Turro and D. A. Tomalia, *Macromolecules* **23**, 910 (1990).
5. G. Caminati, N. Turro and D. Tomalia, *J. Am. Chem. Soc.* **112**, 8515 (1990).
6. (a) G. N. Stewart and M. A. Fox, *J. Am. Chem. Soc.* **118**, 4354 (1996); (b) N. Tanaka, T. Fukutome, T. Tanigawa, K. Hosoya, K. Kimata, T. Araki and K. Unger, *J. Chromatogr. A* **699**, 331 (1995).
7. D. A. Tomalia, H. Baker, J. Dewald, M. Hall, G. Kallos, S. Martin, J. Roeck, J. Ryder and P. Smith, *Macromolecules* **19**, 2466 (1986).
8. M. F. Ottaviani, S. Bossmann, N. Turro and D. Tomalia, *J. Am. Chem. Soc.* **116**, 661 (1994).
9. N. Tanaka, T. Fukutome, K. Hosoya, K. Kimata and T. Araki, *J. Chromatogr. A* **716**, 57 (1995).
10. J. Aaron, A. Tine and M. Gaye, *Spectrochimia Acta, Part A* **47**, 419 (1991).
11. E. Breitmaier, Structure Elucidation by NMR in Organic Chemistry. Wiley, New York (1993).
12. C. Reichardt, in Solvents and Solvent Effects in Organic Chemistry, 2nd ed. VCH, Boca Raton, FL (1990).
13. C. S. Wilcox, in Frontiers in Supramolecular Organic Chemistry and Photochemistry, edited by H. Schneider and H. Durr, pp. 232–245. VCH, Boca Raton, FL (1991).
14. J. Joules, K. Mills and G. Smith, in Heterocyclic Chemistry, 3rd ed. p. 120. Chapman and Hall, London (1995).
15. R. Foster, in Organic Charge Transfer Complexes, edited by A. Blomquist, pp. 210–230. Academic Press, London (1969).
16. M. Joesten and L. J. Schaad, Hydrogen Bonding, p. 173. Marcel Dekker, New York (1974).
17. (a) M. J. Kamlet, J. L. Abboud and R. W. Taft, *J. Am. Chem. Soc.* **99**, 6027 (1977); (b) R. W. Taft and M. J. Kamlet, *J. Am. Chem Soc.* **98**, 2886 (1976); (c) M. J. Kamlet, J. L. Abboud, M. H. Abraham and R. W. Taft, *J. Org. Chem.* **48**, 2877 (1983).